Wave Attenuation due to Vegetation Using the Fully Nonlinear Boussinesq Model

Yu-Lin Tsai, DPRI, Kyoto University, tsai.yulin.6t@kyoto-u.ac.jp
Che-Wei Chang, DOE, the University of Rhode Island, chewei.chang@uri.edu
Nobuhito Mori, DPRI, Kyoto University, mori@oceanwave.jp

INTRODUCTION

Vegetation has a protective function against coastal hazards and also been recognized as a green infrastructure (i.e., nature-based solutions) in coastal and ocean engineering. One notable coastal vegetation is mangroves, which not only protect coastal communities from tsunamis (Danielsen et al., 2005) but also mitigate erosion and climate change (Duke et al., 2014). Hence, more attention has been paid in the recent two decades.

Mangroves are also featured by their prop roots, essential in determining resistance forces to waves (i.e., Maza et al., 2019; Chang et al., 2022). Though the shape of mangroves' roots has been considered in the lab, its effect on wave modeling has not been investigated clearly, especially in the phase-resolving regime. Thus, this study develops a vegetation module onto a fully nonlinear Boussinesq-type wave model, balanced by accuracy and efficiency, for wave attenuation modeling. Wave attenuations by idealized cylinders and Rhizophora apiculate mangroves are showcased in this study.

METHODOLOGY

This study implements the vegetation module onto the fully nonlinear Boussinesq-type wave model (FUNWAVE), which was developed by Chen (2006) and Shi et al. (2012) and is accurate to $O(\mu^2)$ in the wave dispersive effect. Using the perturbation approach, the horizontal velocities $\boldsymbol{u}(z)$ can be expanded as

$$\boldsymbol{u}(z) = \boldsymbol{u_\alpha} + (z_\alpha - z)\nabla\left(\nabla\cdot(h\boldsymbol{u_\alpha})\right) + \frac{1}{2}(z_\alpha^2 - z^2)\nabla(\nabla\cdot\boldsymbol{u_\alpha}) \quad (1)$$

where $\boldsymbol{u_\alpha}$ is the horizontal velocity at the reference level z_α (Kennedy et al., 2001), z is the vertical location, and h is the still water depth. Here, the vegetation-induced resistance is considered as momentum dissipative drag and inertia force terms. Using the reference velocities, the vegetation-induced dissipation term is described as

$$\boldsymbol{R_V} = -\frac{N}{2(h+\eta)}C_D A_{tree}\boldsymbol{u_\alpha}|\boldsymbol{u_\alpha}| - \frac{N}{(h+\eta)}C_M V_{tree}\frac{\partial \boldsymbol{u_\alpha}}{\partial t} \quad (2)$$

in which, N is the forest density, (C_D, C_M) are drag and inertia coefficients, t denotes time, and η is the free surface elevation. Here, we call this the partial approximation approach. In contrast, when introducing the expanded horizontal velocities to the dissipation term, the full integration approach is proposed here:

$$\boldsymbol{R_V} = -\frac{N}{2(h+\eta)}C_D\int_{-h}^{\min(h_v-h,\eta)}\boldsymbol{u}|\boldsymbol{u}|dA_{tree} - \frac{N}{(h+\eta)}C_M\int_{-h}^{\min(h_v-h,\eta)}\frac{\partial \boldsymbol{u}}{\partial t}dV_{tree} \quad (3)$$

h_v is the stem height. The tree's shape is considered: (A_{tree}, V_{tree}) are the projected area and volume integrated from the bottom to the still water level; (dA_{tree}, dV_{tree}) are the projected area and volume varied along the z-axis. Note that these two approaches are extended following Chakrabarti et al. (2017), but we include the inertia force term. The visualization of these two approaches is presented in **Figure 1**.

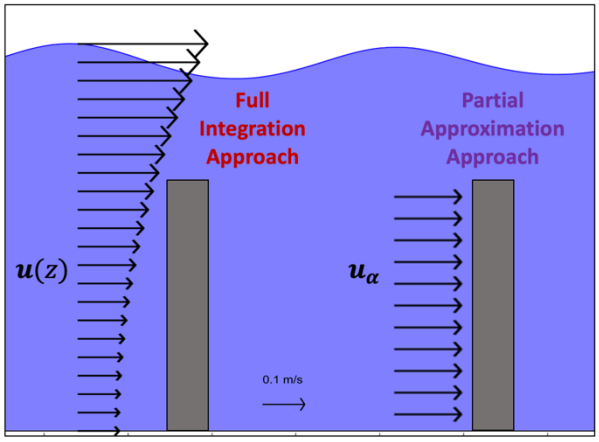

Figure 1 - Sketch of the full integration and partial approximation approaches in vegetation-induced resistance.

IDEALIZED CYLINDER CASE

Wave attenuation in submerged and emergent cylinders is tested, and the model results are compared with Dalrymple et al. (1984)'s analytical solution. Here, we only present the submerged cylinder case. The computational domain is 35 m long with the sponge layers at the two ends of the domain, which is 8 m long. The internal wavemaker is located at 10 m. The incident wave amplitude is 0.025 m, and the wave period is 1.2 sec. The idealized cylinder is assumed, which has a diameter of 0.02 m and a stem height of 0.25 m. The forest density is 500.0 stem/m^2. The width of vegetated areas is 10 m, beginning 12.5 m away from the internal wavemaker.

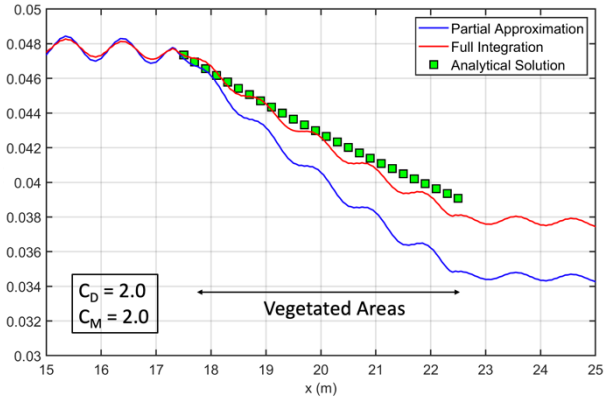

Figure 2 - Example of wave attenuation by submerged cylinders.

Figure 2 shows wave attenuations by the submerged cylinders. In this case, C_D and C_M are set as 2.0. In the comparison, the attenuation using the full integration approach is close to the analytical solution, implying a similar wave damping pattern. However, the partial approximation approach tends to underestimate the wave heights than the analytical solution.

MANGROVE CASE

Wave attenuation by mangroves (i.e., non-uniform vegetation) is tested following the experimental setup of Chang et al. (2022). **Figure 3** shows the mangrove tree's vertical profiles, representing the nineteen-year-old Rhizophora apiculate mangrove in Vietnam. This information is used in simulating wave attenuations.

The computational domain is 61.5 m long with the sponge layers at the two ends. However, as the linear wavemaker is employed, an artificial 3:100 slope is added to generate waves smoothly (Chakrabarti et al., 2017). The width of mangrove areas is 4.07 m. The forest density is 29.4 stem/m^2, the diameter of the breast height is 1.0 cm, and the stem height of mangroves is 19.5 cm.

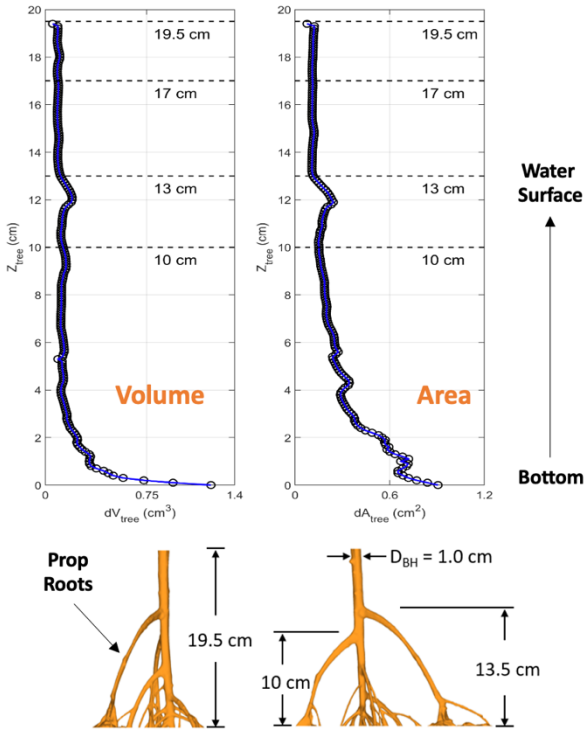

Figure 3 - Vertical profiles of the mangrove and replicated model in the lab experiment.

Wave attenuation due to mangroves with ±50% drag and inertia coefficient formulations is shown in **Figure 4**. The bottom friction is included (the Manning's coefficient is 0.013). The wave period is 1.7 s, the wavelength is 2.108 m, and the still water depth is 17 cm. In the simulations, the drag and inertia coefficients are spatially varied according to the Reynolds (R_e) and Keulegan-Carpenter (K_c) numbers. As shown in **Figure 4**, the trend of simulated attenuation fits the lab measurements. We also found that the simulated wave attenuation varies more significantly when closer to the end of the mangrove forest. We have tested wave attenuations on different water depths, and they will be presented in ICCE 2024.

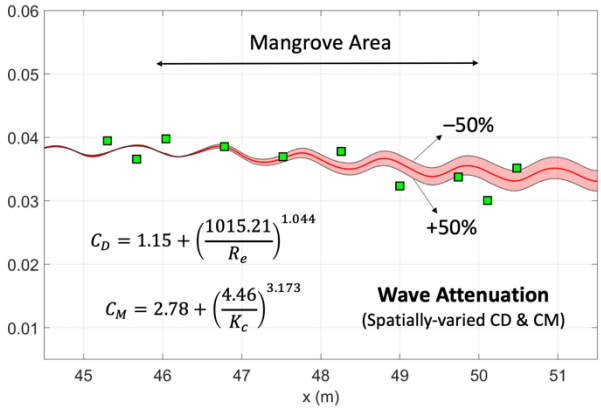

Figure 4 - Wave attenuation by mangroves using the full integration approach on the still water depth of 17 cm.

CONCLUDING REMARKS

This study has developed a vegetation module onto a fully nonlinear Boussinesq-type wave model (FUNWAVE-VEG). Two approaches for calculating vegetation-induced resistance to waves were considered: the partial approximation approach (i.e., the reference velocity method) and the full integration approach (i.e., the perturbation velocity method). The cylinder cases were tested, and we found the partial approximation approach tends to overpredict wave attenuation than the full integration approach in the submerged cylinder case. Furthermore, the wave attenuations due to mangroves were explored. The mangrove tree's geometry was considered in the simulations. The trend of simulated attenuation fits the lab measurements, but the variations become larger when closer to the end of the mangrove forest. By presenting this numerical model package, we hope to pay the way for simulating wave attenuations with complicated vegetation and future real-scale applications.

ACKNOWGEMETNS

This research is supported by the STRAPS-BRICC project, funded by JST (Japan Science and Technology Agency) and JICA (Japan International Cooperation Agency).

REFERENECES

Chakrabarti, A., Brandt, S. R., Chen, Q., & Shi, F. (2017). JGR-Oceans, 122(5), 3861-3883.

Chang, C., Mori, N., Tsuruta, N., Suzuki, K., & Yanagisawa, H. (2022). JGR-Oceans, 127(6).

Chen, Q. (2006). JEM, 132(2), 220-230.

Dalrymple, R. A., Kirby, J. T., & Hwang, P. A. (1984). JWPCOE, 110(1), 67-79.

Danielsen, F. et al. (2005). Science, 310(5748), 643-643.

Duke, N. et al. (2014): The importance of mangroves to people: a call to action.

Kennedy, A. B., Kirby, J. T., Chen, Q., & Dalrymple, R. A. (2001). 33(3), 225-243.

Shi, F., Kirby, J. T., Harris, J. C., Geiman, J. D., & Grilli, S. T. (2012). Ocean Modelling, 43, 36-51.

Maza, M., Lara, J. L., & Losada, I. J. (2019). Advances in Water Resources, 131, 103376.